Neuroscience 348 (2017) 11–22

MODULATION OF THE SENSORIMOTOR SYSTEM BY SUSTAINED MANUAL PRESSURE STIMULATION

PAVEL HOK,[a,b]* JAROSLAV OPAVSKÝ,[c] MIROSLAV KUTÍN,[d,e] ZBYNĚK TÜDÖS,[f,g] PETR KAŇOVSKÝ[a,b] AND PETR HLUŠTÍK[a,b]

[a] *Department of Neurology, Faculty of Medicine and Dentistry, Palacky University Olomouc, I. P. Pavlova 185/6, Olomouc CZ-77520, Czech Republic*

[b] *Department of Neurology, University Hospital Olomouc, I. P. Pavlova 185/6, Olomouc CZ-77520, Czech Republic*

[c] *Department of Physiotherapy, Faculty of Physical Culture, Palacky University Olomouc, tř. Míru 671/117, Olomouc CZ-77111, Czech Republic*

[d] *KM KINEPRO PLUS s.r.o., Horní lán 1328/6, Olomouc CZ-77900, Czech Republic*

[e] *Department of Physiotherapy, Faculty of Health Sciences, Palacky University Olomouc, Hněvotínská 976/3, Olomouc CZ-77515, Czech Republic*

[f] *Department of Radiology, Faculty of Medicine and Dentistry, Palacky University Olomouc, I. P. Pavlova 185/6, Olomouc CZ-77520, Czech Republic*

[g] *Department of Radiology, University Hospital Olomouc, I. P. Pavlova 185/6, Olomouc CZ-77520, Czech Republic*

Abstract—In Vojta physiotherapy, also known as reflex locomotion therapy, prolonged peripheral pressure stimulation induces complex generalized involuntary motor responses and modifies subsequent behavior, but its neurobiological basis remains unknown. We hypothesized that the stimulation would induce sensorimotor activation changes in functional magnetic resonance imaging (fMRI) during sequential finger opposition. Thirty healthy volunteers (mean age 24.2) underwent two randomized fMRI sessions involving manual pressure stimulation applied either at the right lateral heel according to Vojta, or at the right lateral ankle (control site). Participants were scanned before and after the stimulation when performing auditory-paced sequential finger opposition with their right hand. Despite an extensive activation decrease following both stimulation paradigms, the stimulation of the heel specifically led to an increase in task-related activation in the predominantly contralateral pontomedullary reticular formation and bilateral posterior cerebellar hemisphere and vermis. Our findings suggest that sustained pressure stimulation of the foot is associated with differential short-term changes in hand motor task-related activation depending on the stimulation. This is the first evidence for brainstem modulation after peripheral pressure stimulation, suggesting that the after-effects of reflex locomotion physiotherapy involve a modulation of the pontomedullary reticular formation.

Key words: functional magnetic resonance imaging, physical stimulation, neurophysiotherapy, movement, brainstem, cerebellum.

INTRODUCTION

Peripheral afferent stimulation has been used to induce experimental plasticity of the motor system and has become an important component of techniques to improve or restore human motor function (Powell et al., 1999). Most widely studied types of peripheral stimulation include nerve stimulation by electrical current, which is easy to control and administer (Chipchase et al., 2011). A prominent modulation of task-related activity in the sensorimotor cortex was repeatedly observed after transcutaneous electrical or magnetic stimulation (Golaszewski et al., 2004; Wu et al., 2005; Gallasch et al., 2015). Natural modalities of peripheral stimulation, such as tactile, pressure or proprioceptive, have been investigated less extensively (Rosenkranz and Rothwell, 2003), even though they represent essential elements of clinical rehabilitation techniques and procedures, such as the "reflex locomotion" (Vojta, 1973; Vojta and Peters, 2007).

The reflex locomotion technique, also known as Vojta method, utilizes sustained manual pressure stimulation of specific points on the skin surface to gradually evoke a stereotypic widespread motor response, i.e., an asymmetrical pattern of tonic muscle contractions in both sides of the neck, trunk and limbs (Vojta, 1973). After the stimulation, changes in motor behavior have been observed for at least 30 min (Vojta and Peters, 2007). Despite ongoing clinical use of the reflex locomotion therapy (Lim and Kim, 2013), there is limited knowledge of its neurobiological basis since the available evidence is mostly based on clinical observation studies (Vojta and Peters, 2007). Based on comparisons with other human

*Correspondence to: P. Hok, Department of Neurology, Faculty of Medicine and Dentistry, Palacky University Olomouc, I. P. Pavlova 185/6, Olomouc CZ-77520, Czech Republic. Fax: +420-585-413-841.

E-mail addresses: pavel.hok@upol.cz (P. Hok), jaroslav.opavsky@upol.cz (J. Opavský), mirek.kutin@kinepro.cz (M. Kutín), zbynek.tudos@fnol.cz (Z. Tüdös), petr.kanovsky@fnol.cz (P. Kaňovský), phlustik@upol.cz (P. Hluštík).

Abbreviations: AS, stimulation of the ankle; BA, Brodmann's area; BOLD, blood oxygenation level-dependent; CPG, central pattern generators; fMRI, functional magnetic resonance imaging; HS, stimulation of the heel; MNI, Montreal Neurological Institute; MRI, magnetic resonance imaging; PMRF, pontomedullary reticular formation; SD, standard deviation; SFO, sequential finger opposition; VAS, visual analog scale.

http://dx.doi.org/10.1016/j.neuroscience.2017.02.005
0306-4522/

involuntary motor responses, such as tonic neck reflex (Magnus and de Kleijn, 1912), and responses elicited due to engagement of the central pattern generators (CPG) in vertebrate animals (Grillner and Wallén, 1985), the motor response to stimulation according to Vojta has been suggested to originate from the midbrain or neighboring structures (Vojta, 1973; Laufens et al., 1991). The concept of the CPG in the human sensorimotor system has recently gained support as the brainstem structures have been increasingly associated with human locomotion and postural control (Jahn et al., 2008; la Fougère et al., 2010; Takakusaki, 2013). Although there is no direct evidence that peripheral pressure stimulation according to Vojta (1973) involves the brainstem CPG, pressure stimulation applied at analogous sites in cats, i.e., at foot pads or chest, leads to similar complex tonic reflexes (Hongo et al., 1990) or modulation of posture-dependent muscle activity (D'Ascanio et al., 1986), respectively. In humans, cutaneous pressure input via slowly adapting afferents from the foot soles participates in postural control as well (Kavounoudias et al., 2001).

Considering the available neurophysiological (Gallasch et al., 2015), imaging (Golaszewski et al., 2004; Wu et al., 2005; Gallasch et al., 2015) and clinical (Vojta, 1973; Lim and Kim, 2013) evidence, we propose that extended peripheral pressure stimulation would cause modulation of the motor system that outlasts the stimulation itself. Presumably, one possible modulation site could be expected in the sensorimotor cortex (Gallasch et al., 2015). However, we hypothesize that stimulation according to Vojta primarily modulates the brainstem structures where the generator of the motor response to the stimulation has been suggested (Laufens et al., 1991). Lastly, we hypothesize that motor control will be differentially modulated by stimulating the empirical foot zone according to Vojta when compared to stimulation of a nearby silent control site on the foot.

We have employed functional magnetic resonance imaging (fMRI) with a paced sequential finger opposition (SFO) task repeated before and after sustained pressure stimulation at either an active or control site on the foot to test our hypotheses. The presented findings suggest that sustained pressure stimulation of the foot is associated with differential short-term changes in hand motor task-related activation in the brainstem and cerebellum that depend on the stimulation site. The pontomedullary reticular formation is speculated to play a key role in reflex locomotion physiotherapy.

EXPERIMENTAL PROCEDURES

Participants

Thirty healthy volunteers enrolled in this study (16 females and 14 males, mean age 24.20, standard deviation [SD] 1.92). The subjects were university students who were naïve to Vojta therapy (Vojta and Peters, 2007), had no history of any neurological condition, and had no signs of motor disability upon enrollment. Three participants were left-handed and 27 were right-handed as assessed by the Edinburgh handedness inventory (Oldfield, 1971). The study was carried out in accordance with World Medical Association Declaration of Helsinki. Written informed consent was obtained from all participants prior to their inclusion in the study and the study was approved by the Ethics Committee of the University Hospital and the Faculty Medicine Palacky University in Olomouc, approval number 9.4.2013.

Task and procedures

Each fMRI session included 2 functional imaging acquisitions during 6-min right hand SFO. The task was performed in 15-s blocks alternating with 15-s rest. Participants were asked to tap sequentially the right index, middle, ring and little finger against the thumb, and to repeat the sequence throughout the block. The performance was paced at 2 Hz by high-pitch (500 Hz) tones delivered using MR-compatible headphones. The rest was marked by low-pitch tones (300 Hz) of the same volume and pace. The motor task was trained briefly outside the scanner room before every session.

The two SFO runs were separated by 20 min of intermittent manual pressure stimulation delivered by an experienced therapist (M.K.) and by subsequent 8-min rest. The pressure stimulation was applied with the therapist's thumb either at the right lateral heel zone (heel stimulation, HS) according to Vojta (1973), or at the control site at the right lateral ankle (ankle stimulation, AS), both sites within the same dermatome (Foerster, 1933) on the skin covering bony structures. In effect, the SFO was tested before (condition H1 or A1) and after the stimulation (condition H2 or A2). The therapist was instructed to use the same pressure routinely used during physiotherapy according to Vojta, while the participants were lying prone in the scanner bore throughout the session. The applied pressure was recorded during the stimulation using a custom-made MR-compatible calibrated pressure monitor (incorporating a FlexiForce pressure sensor, Tekscan, South Boston, MA, USA). The body position and stimulation duration, as well as usage of a single stimulation site, were chosen to elicit only partial motor response (Vojta and Peters, 2007), avoiding gross movements in the scanner bore and head displacement.

After each session, participants completed a visual analog scale for pain (VAS) form with 0 (no pain) and 10 (worst possible pain) marked as the extreme values to assess whether the stimulation evoked painful sensations (Joyce et al., 1975). The pain scores for HS and AS were compared using Wilcoxon's two-sample signed rank test.

Each participant underwent two fMRI sessions, each involving either HS or AS. The order of the sessions was randomized and counter-balanced, and the participants were not informed in advance that the stimulation would be performed in one of two different sites. The sessions were scheduled at least 1 week apart, the median time interval between sessions was 70 days (range 7–294 days).

Data acquisition

Magnetic resonance imaging (MRI) data were acquired using 1.5-Tesla scanners (Siemens Avanto and

Siemens Symphony, Erlangen Germany) with standard 12-channel head coils. The scanning schedule was counter-balanced to account for any possible differences due to the scanner used. The subject's head was immobilized with cushions to assure maximum comfort and minimize head motion. The MRI protocol included functional T_2^*-weighted blood oxygenation level-dependent (BOLD) images during task performance and control state. BOLD images were acquired with gradient-echo echo-planar imaging (EPI; 30 axial slices parallel to the anterior commissure-posterior commissure [AC-PC] line, 5 mm thick, repetition time/echo time = 2500/41 ms, flip angle 80°, field of view = 220 mm, matrix 64×64) to provide $3.4 \times 3.4 \times 5.0$ mm resolution. In total, 144 images were acquired per each 6-min functional run. Gradient-echo phase and magnitude fieldmap images were acquired to allow correction of the echo planar imaging distortions. Anatomical high-resolution three-dimensional magnetization-prepared rapid acquisition with gradient echo (MPRAGE) scan was acquired to provide the anatomical reference. In-plane fluid-attenuated inversion recovery (FLAIR) images were used to screen for unsuspected brain lesions.

Data analysis

The fMRI data were processed using FEAT (FMRI Expert Analysis Tool) Version 6.00, part of FSL (FMRIB's Software Library, www.fmrib.ox.ac.uk/fsl) (Jenkinson et al., 2012). Standard pre-processing was applied, including spatial smoothing using a Gaussian kernel with 8.0-mm full width at half maximum (FWHM) and high-pass temporal filtering with sigma = 45.0 s. Time series statistical analysis included a temporal derivative of the main effect to account for slice timing shift and functional data were registered non-linearly to the Montreal Neurological Institute (MNI) 152 standard space (Grabner et al., 2006). The fMRI data were then visually checked for susceptibility artifacts and two subjects were excluded due to an excessive signal loss in the brainstem. Three subjects were excluded due to a maximum frame-wise head displacement exceeding 3 mm in a single run as estimated during motion correction. The final sample thus consisted of 25 subjects (14 females, 11 males, 22 right-handers).

For an additional analysis, motion-related artifacts were removed from each time series using ICA-AROMA tool and nuisance signal regressors of mean signal from cerebral ventricles and white matter were added to the model (Pruim et al., 2015a, 2015b). The following steps were performed for both original, and de-noised time series.

The group-level general linear model consisted of four conditions: SFO before and after the HS (conditions H1 and H2, respectively), and SFO before and after the AS (A1 and A2, respectively). Additionally, two subset conditions $H1^*$ and $A1^*$ were defined, including only datasets acquired at the first session. Using these conditions, five group post hoc contrasts were constructed, including (1) a pooled group-wise activation image (H1 + H2 + A1 + A2), (2) differences between the baseline conditions at the first session ($H1^*$ v. $A1^*$), and (3) differences between the task repetitions regardless of stimulation type (H1 + A1 v. H2 + A2). The main research questions were assessed using (4) a two-by-two interaction between the condition and the task repetition (H2 − H1 v. A2 − A1). An additional linear covariate modeled individual differences in self-rated pain intensity (condition H–condition A), yielding statistical maps of (5) pain intensity effect on the interaction. All within-subject contrasts were first computed using a fixed effects analysis, and the resulting parameter estimates (beta values) and variance were then carried over to the third-level analysis. The primary outcome measure was significant *F*-test in contrasts 4 and 5, followed by post hoc voxel-wise and cluster-wise analyses to assess the directionality of the significant *F*-test effects.

The random effects analysis was conducted using FLAME (FMRIB's Local Analysis of Mixed Effects) stage 1 (Woolrich et al., 2004). The whole-brain analysis was constrained to the MNI standard brain mask (Grabner et al., 2006) excluding white matter voxels according to the Harvard–Oxford probabilistic atlas (Desikan et al., 2006) using a conservative probability threshold of 95%. The masked *Z* (Gaussianized T) statistic images were thresholded using clusters determined by $Z > 2.3$ and a corrected cluster significance threshold of $p < 0.05$ (Worsley, 2001). The post hoc *t*-tests in contrast 4 were carried out within the significant *F*-test clusters and thresholded voxel-wise at corrected significance level $p < 0.05$. The thresholded maps were objectively labeled based on Harvard–Oxford Cortical and Subcortical Structural Atlases (Desikan et al., 2006), and Probabilistic Cerebellar Atlas (Diedrichsen et al., 2011). Cytoarchitectonic labels were provided by Jülich Histological Atlas (Eickhoff et al., 2007).

A confirmatory third-level analysis was carried out for contrast 4 using non-parametric Conditional Monte Carlo permutation testing implemented in Randomise v2.9 (Winkler et al., 2014). An identical design with the pain intensity covariate was employed. Ten thousand permutations were performed using sign-flipping to estimate the null distribution of the maximum cluster mass under the cluster forming threshold of $t > 3.0$.

A post hoc region of interest (ROI) analysis was performed to investigate the contribution of each condition to the overall interaction in contrasts 4 and 5 and to assess the correlation with the self-reported pain intensity. First, significant voxels in each cluster were identified using a post hoc voxel-wise *t*-test carried out within the *F*-test mask and the resulting mask was transformed back to the individual subject space. Next, average (mean) *Z* scores and percent signal change (% SC) values across the ROI were extracted from each individual single-subject statistical map in the specified mask using the Featquery tool, part of FSL. The obtained values were plotted and compared group-wise using paired Wilcoxon's signed rank test and correlated with the pain intensity covariate using Spearman's correlation coefficient.

RESULTS

Behavioral data

In all subjects, the therapist reported discrete irregular muscle contractions in the stimulated extremity during stimulation, but no gross limb or trunk movements were observed.

For technical reasons, pressure recordings were only obtained in 15 subjects. The mean pressure during the HS was 22.33 N (SD = 11.64 N), and it was 26.45 N (SD = 9.72 N) during the AS. The difference was not significant ($p = 0.32$, two-sample t test). A paired t-test was possible in 11 subjects, yielding an insignificant difference ($p = 0.22$, mean difference HS–AS = −3.94 N, SD = 9.96 N).

During the HS, the median reported pain intensity (VAS) was 1.85 (range 0–6.9), while it was 0.90 (range 0–5.5) during the AS. The HS was thus associated with significantly higher pain intensity than the AS ($p < 0.01$, Wilcoxon's signed rank test). The median difference was 1.25 (range −5.0–6.4).

Imaging results

Mean fMRI activation during sequential finger opposition (SFO). As illustrated in Fig. 1, the analysis of mean activation pooled across all conditions (H1, H2, A1 and A2) yielded a single significant cluster representing predominantly contralateral (left) frontoparietal and subcortical sensorimotor areas, as well as predominantly contralateral midbrain and pons, and ipsilateral (right) cerebellar hemisphere and vermis.

Difference between baseline conditions. The t-test comparing the condition H1* and condition A1* (i.e., the baseline at the first session) did not show any significant difference at the whole-brain level.

Mean activation difference before and after the stimulation. The paired t-test before and after the stimulation averaged across both sessions showed that there was no significant mean activation increase after the stimulation. However, it revealed a decrease in activation in several areas, including the bilateral supplementary motor area (SMA) and lateral premotor cortex (lateral BA 6); superior parietal lobule (mainly BA 7); primary somatosensory cortex (mainly BA 2); intracalcarine (V1, V2) and ventral visual occipital cortex (V4); cerebellar hemispheres (mainly lobule VI) and vermis (blue in Fig. 2). Significant clusters are summarized in Table 1.

Two-by-two interaction between condition and task repetition. The F-test of two-by-two interaction between the condition and repetition (H2–H1 v. A2–A1) yielded a single significant cluster in the left ventral pons and bilateral pontomedullary junction at the base of the 4th ventricle. The cluster extended to the bilateral cerebellar hemispheres and vermis (mainly bilateral lobule IX and less right lobule VIII), bilateral interposed and the right dentate nucleus (red-yellow in Fig. 2), while there was no significant interaction in the cerebral cortex, thalamus or basal ganglia. The significance of the cluster in the brainstem was not affected by adding the pain intensity covariate and the same cluster was also observed in the confirmatory analysis using non-parametric thresholding (Randomise). Although the data de-noising using ICA-AROMA (Pruim et al., 2015a,b) led to decrease in the F-test cluster volume in each analysis, it remained significant in most analyses. These results are summarized in Table 2. To maintain clarity, only the results of original data analysis are further presented and discussed. The F-test cluster resulting from parametric analysis of interaction with pain intensity covariate is further referred to as the hindbrain cluster. The post hoc voxel-wise t-test within the hindbrain cluster showed that only the contrast H2–H1 > A2–A1 was significant.

The effect of pain intensity yielded one cluster encompassing the right inferior frontal gyrus (BA 45), anterior insular cortex, frontal operculum, and frontal orbital cortex, as shown in green in Fig. 2 and Table 2. This cluster is further referred to as insulo-opercular cluster.

Post-hoc ROI analysis. The ROI analysis of average Z scores derived from the hindbrain cluster (contrast 4) showed that the activation increased significantly after the HS (H2–H1: median Z difference = 0.63, $p < 0.001$, uncorrected), and decreased significantly after the AS (A2–A1: median Z difference = −1.1,

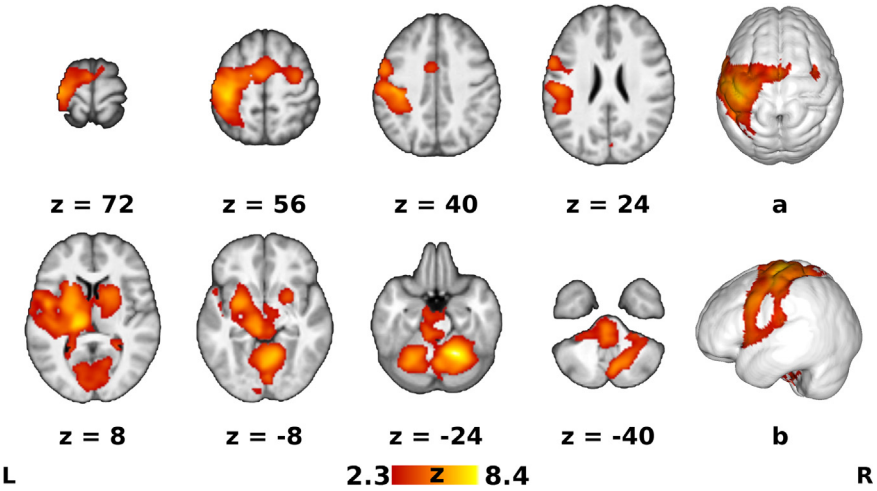

Fig. 1. Mean activation during sequential finger opposition. *Black-and-white figure in print.* The red-yellow Z statistical overlay represents mean activation during the right hand sequential finger opposition pooled across all runs and sessions. The image was superimposed on top of a gray-scale mean T1-weighted background image. Clusters of activation were determined by $Z > 2.3$ and thresholded at corrected $p < 0.05$. The axial slices are numbered over the Z axis of the Montreal Neurological Institute (MNI) 152 standard space template. Panels a (top view) and b (left lateral view) show the statistical overlay on top of a three-dimensional reconstructed cortical surface. The right is right, according to neurological convention.

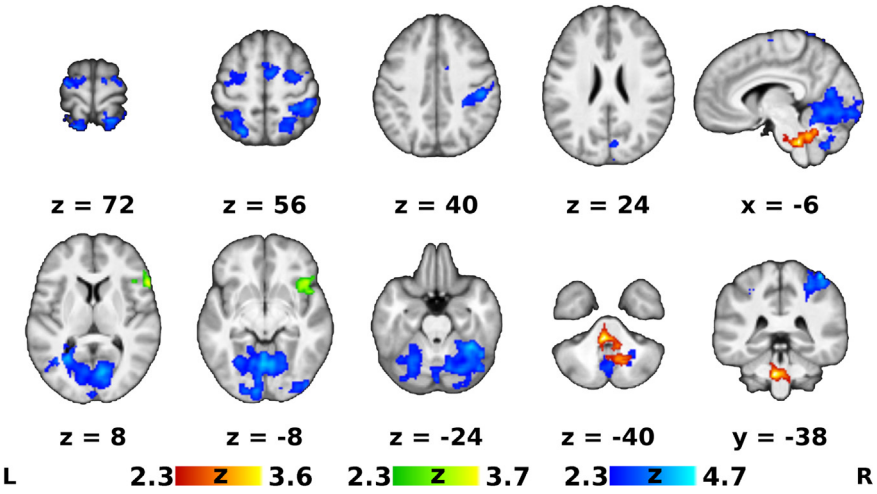

Fig. 2. Mean activation decrease post-stimulation and interaction between condition and repetition. *Black-and-white figure in print.* The blue *Z* statistical overlay represents a decrease in task-related activation after the stimulation common to both conditions, i.e., contrast 3: (H1 + A1)–(H2 + A2). The red-yellow *Z* statistical overlay shows significant *F*-test of interaction between the condition and repetition (contrast 4: H1–H2 v. A1–A2) with the pain intensity covariate. The green *Z* statistical overlay shows the significant *F*-test of the pain covariate effect in the interaction (contrast 5). Remaining conventions see Fig. 1.

$p < 0.001$, uncorrected), see Fig. 3. Likewise, the two effects differed significantly ($p < 0.001$, uncorrected).

In contrast, the insulo-opercular cluster representing the pain intensity effect did not show any significant difference in *Z* scores between the conditions or task repetitions ($p > 0.05$, uncorrected). The post hoc ROI analysis confirmed that the interaction in *Z* scores (H2–H1) > (A2–A1) in the insulo-opercular cluster was negatively correlated with the pain intensity difference (H–A), see Fig. 4. The ρ was -0.54 ($p = 0.006$, uncorrected). In other words, the higher the perceived pain during the stimulation, the larger the decrease in the BOLD response in the insulo-opercular cluster after the stimulation (i.e., in H2 or A2) relative to baseline (H1 or A1). However, the activation differences between the task repetitions (i.e., H2–H1 and/or A2–A1) were not significantly correlated with the average pain intensity in H or A condition ($p > 0.05$, uncorrected). Likewise, none of these correlations were significant in the hindbrain cluster ($p > 0.05$, uncorrected).

DISCUSSION

Using the SFO as a robust task activating multiple levels of the sensorimotor system (red-yellow in Fig. 1), we have demonstrated that despite an extensive decrease in activation following both stimulation paradigms (blue in Fig. 2), the sustained pressure stimulation of the heel (HS) differentially modulated the task-related activation in the predominantly contralateral pons and ipsilateral cerebellum (red-yellow in Fig. 2). The following sections discuss putative underlying mechanisms and the implications of these results.

Average activation during SFO

The cortical, subcortical and cerebellar areas activated during SFO correspond well to previous reports of motor control of complex finger tasks (Solodkin et al., 2001). Despite the fact that the brainstem areas observed in this study (Fig. 1) are reported less frequently during skilled hand movement, midbrain/pons regions have been shown to engage during imagery of motor hand movement (Ueno et al., 2010; Sauvage et al., 2011). Moreover, pontine reticular formation participates in motor control of the forelimbs in animal studies (Sharp and Ryan, 1984).

Activation decrease post-stimulation

All of the areas showing activation decrease post-stimulation (blue in Fig. 2) have been associated with control of complex finger movements (Solodkin et al., 2001) and their activation is known to decrease when repeating the same motor task, both over shorter (Kincses et al., 2008) and longer time scales (Steele and Penhune, 2010). These decreases have therefore been mostly interpreted as early stages of motor learning (Steele and Penhune, 2010) which is also the most likely explanation of the activation decrease upon repeating the same finger motor task in the present study. With the present design lacking another control group with simple task repetition (i.e., no foot stimulation between the first and second finger movement task), we cannot exclude the possibility that at least some of the decreases were related to nonspecific after-effects of peripheral stimulation (of a different body part), even though such effects have not been reported so far.

Site-specific effects of stimulation

An interaction between the stimulation site and the task repetition was found in the brainstem and cerebellum, whereas no such effect was observed in the cerebral cortex. In contrast, previous functional imaging studies have shown that other modalities of peripheral stimulation, such as peripheral magnetic stimulation of the forearm between two repetitions of a finger movement task (Gallasch et al., 2015), resulted in increased activation of the contralateral sensorimotor cortex. We suggest that the absence of such an effect on the cortex in this study may result from the distance between the sensorimotor representations of the stimulated foot and of the fingers involved in the SFO.

The reported effect on hindbrain structures, on the other hand, may reflect less topographical and more diffuse arrangement of afferent or efferent pathways in the hindbrain, which are not necessarily related to the motor control of a single extremity.

Here, the site-specific interaction was found mainly in the bilateral posterior cerebellar hemispheres and vermis, as well as in the left ventral and bilateral dorso-caudal pons, i.e., in areas likely corresponding to the left

Table 1. List of significant clusters in comparison before and after the stimulation (contrast 3)

Contrast	Anatomical atlas labels[a]	Cytoarchitectonic atlas labels[a]	Volume [cm^3]	Cluster p	Z_{max}	Z_{max} MNI coordinates [x, y, z (mm)]
Contrast 3: (H1 + A1) > (H2 + A2) – original data	22.9% R cerebellar hemisphere (10.7% right VI) 15.7% L cerebellar hemisphere (7.3% left VI) 14.3% L lingual gyrus 10.3% R lingual gyrus 8.6% L occipital fusiform gyrus 6.4% R occipital fusiform gyrus 6.1% L intracalcarine cortex 6.0% R intracalcarine cortex 6.0% R temporo-occipital fusiform cortex 5.0% cerebellar vermis	8.0% L visual cortex V1 (BA17) 7.7% R visual cortex V1 (BA17) 7.4% L visual cortex V4 6.3% L visual cortex V2 (BA18) 5.6% R visual cortex V2 (BA18)	98.9	< 0.001	4.75	−26, −68, −18
	38.6% R superior parietal lobule 30.5% R postcentral gyrus 16.3% R lateral occipital cortex 13.9% R supramarginal gyrus	33.4% R superior parietal lobule (BA7) 25.9% R primary somatosensory cortex (BA2) 15.1% R inferior parietal lobule 8.3% R primary somatosensory cortex (BA1) 7.7% R superior parietal lobule (BA5)	17.6	< 0.001	4.59	42, −40, 64
	38.6% R precentral gyrus 31.3% R SMA 17.0% R superior frontal gyrus	93.8% R premotor cortex (BA6) 5.5% L premotor cortex (BA6)	11.3	< 0.001	3.58	16, −14, 68
	65.7% L superior parietal lobule 32.7% L lateral occipital cortex	78.5% L superior parietal lobule (BA7) 11.2% L primary somatosensory cortex (BA2)	10.3	< 0.001	4.50	−30, −56, 64
	49.6% L precentral gyrus 35.7% L superior frontal gyrus 9.0% L middle frontal gyrus 5.7% L SMA	97.4% L premotor cortex (BA6)	6.0	0.017	3.47	−42, 0, 60

Abbreviations: BA – Brodmann area; L – left; N/A – not available; MNI – Montréal Neurological Institute; R – right; SMA – supplementary motor area (also juxtapositional lobule cortex); Z_{max} – maximum Z score.

[a] Anatomical and cytoarchitectonic labels are provided including the proportion of labeled voxels. Only labels containing at least 5% of activated voxels are provided. Note that cerebellar labels may overlap with whole-brain labels and that cytoarchitectonic labels do not cover the whole brain.

Table 2. List of significant *F*-test clusters in the interaction between condition and repetition (contrast 4) and the pain-related effect (contrast 5)

Contrast	Anatomical atlas labels[a]	Cytoarchitectonic atlas labels[a]	Volume [cm^3]	Cluster *p*	Z_{max}	Z_{max} MNI coordinates [*x*, *y*, *z* (mm)]
Contrast 4: (H2–H1 v. A2–A1) without pain covariate (F test) – original data	50.3% brainstem 25.7% R cerebellar hemisphere (15.3% right IX, 7.6% right VIII) 15.4% cerebellar vermis (9.0% vermis IX) 9.2% R dentate nucleus 9.0% L cerebellar hemisphere (7.2% left IX)	N/A	8.17	0.004	3.68	−4, −36, −40
Contrast 4: (H2–H1 v. A2–A1) without pain covariate (F test) – de-noised data	42.0% brainstem 30.6% L cerebellar hemisphere (30.5% left IX) 27.4% cerebellar vermis (16.9% vermis IX, 6.3% vermis X) 26.6% R cerebellar hemisphere (19.4% right IX, 7.1% right VIII)	N/A	4.94	0.034	3.40	−2, −54, −38
Contrast 4: (H2–H1 v. A2–A1) with pain covariate (F test) – original data	51.4% brainstem 25.2% R cerebellar hemisphere (16.0% right IX, 6.7% right VIII) 15.5% cerebellar vermis (8.7% vermis IX) 9.1% R dentate nucleus 8.9% L cerebellar hemisphere (7.1% left IX)	N/A	7.98	0.004	3.64	−6, −38, −40
Contrast 4: (H2–H1 v. A2–A1) with pain covariate (F test) – de-noised data	39.2% brainstem 32.8% R cerebellar hemisphere (18.7% right IX, 13.3% right VIII) 27.7% L cerebellar hemisphere (27.5% left IX) 25.6% cerebellar vermis (16.6 vermis IX, 6.2% vermis X)	N/A	5.06	0.029	3.80	30, −54, −52
Contrast 4: (H2–H1 > A2–A1) with pain covariate (t-test in Randomise) – original data	58.8% brainstem 27.2% R cerebellar hemisphere (17.1% right IX, 7.9% right VIII) 14.2% cerebellar vermis (7.4% vermis X, 5.1% vermis IX) 9.8% R dentate nucleus 8.4% L cerebellar hemisphere (7.9% left IX)	N/A	4.74	0.048	5.27[b]	−4, −38, −42
Contrast 4: (H2–H1 > A2–A1) with pain covariate (*t*-test in Randomise) – de-noised data	45.3% brainstem 30.5% L cerebellar hemisphere (30.5% right IX) 30.3% R cerebellar hemisphere (30.3% right IX) 28.3% cerebellar vermis (20.4% vermis IX, 6.9% vermis X)	N/A	3.25	0.081[c]	4.49[b]	−8, −50, −36
Contrast 5: Correlation of (H2–H1 v. A2–A1) with pain intensity difference (H > A) – original data	37.5% R inferior frontal gyrus, pars triangularis 20.0% R frontal orbital cortex	56.1% R Broca's area (BA45)	5.55	0.03	3.75	58, 22, 10

(*continued on next page*)

Table 2 (*continued*)

Contrast	Anatomical atlas labels[a]	Cytoarchitectonic atlas labels[a]	Volume [cm^3]	Cluster p	Z_{max}	Z_{max} MNI coordinates [x, y, z (mm)]
	17.9% R insular cortex 10.8% R frontal operculum cortex 7.6% R inferior frontal gyrus, pars opercularis 5.8% R temporal pole					

Abbreviations: BA – Brodmann area; L – left; N/A – not available; MNI – Montréal Neurological Institute; R – right; SMA – supplementary motor area (also juxtapositional lobule cortex); Z_{max} – maximum Z score.

[a] Anatomical and cytoarchitectonic labels, including the proportion of labeled voxels. Only labels containing at least 5% of activated voxels are provided. Note that cerebellar labels may overlap with whole-brain labels and that cytoarchitectonic labels do not cover the whole brain.

[b] Maximum t score listed instead of Z_{max}.

[c] Cluster was listed despite non-significant. t-Test to allow comparison among performed analyses.

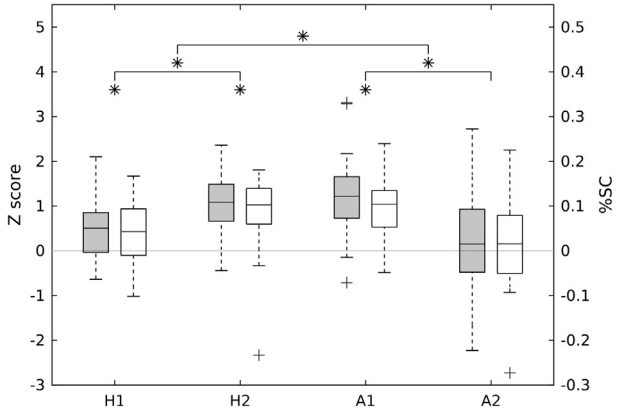

Fig. 3. Post-hoc analysis of significant F-test. *Black-and-white figure in print.* The box plots show average effects of main conditions in individual subjects extracted from the significant voxels in the hindbrain cluster (contrast 4). Gray boxes indicate average Z scores, whereas the white boxes indicate the average percent signal change (%SC) of the same conditions. The conditions are: H1 – before heel stimulation, H2 – after the heels stimulation, A1 – before the ankle stimulation, and A2 – after the ankle stimulation. Each box shows the interquartile range, median (inner horizontal line), extreme (whiskers) and outlier values (crosses). The asterisks above each box and above the horizontal lines indicate conditions and differences where Z scores were significantly different from zero at $p < 0.05$, using Wilcoxon's signed rank test.

pontine nuclei and bilateral lateral pontomedullary reticular formation (PMRF) according to a post-mortem brainstem atlas (Nieuwenhuys et al., 2008).

The post hoc analysis of the interaction indicated that the activation decreased after the AS, likely matching the non-specific extensive BOLD response reduction in other sensorimotor areas due to early motor learning (Steele and Penhune, 2010). In contrast, the opposite effect represented by increased activation after the HS likely reflects specific effects of the peripheral stimulation site as the task execution pace was kept constant across all conditions. Similar activation increase post-stimulation was previously reported in the cerebral cortex (Gallasch et al., 2015). We argue that this effect was not due to the associated pain perceived during the stimulation since the activation in the hindbrain areas did not correlate with the pain intensity and the effect remained significant after adding pain intensity covariate. In fact, contrast 5 (green in Fig. 2) revealed that the task-related activation was modulated by pain intensity in the contralateral (left) anterior insula and frontal operculum, i.e., in areas overlapping with the pain network (Apkarian et al., 2005) as discussed below.

Brainstem

Within the area of significant site-specific stimulation effect, the local maxima were found in the PMRF, which is known to be involved in sensorimotor control. Stimulation of the reticulospinal pathway originating in the PMRF, especially in its lateral part (Takakusaki and Nozu, 2016), elicits bilateral asymmetrical motor patterns in cats (Dyson et al., 2014) and monkeys (Hirschauer and Buford, 2015). In cats, the PMRF has been also shown to contribute to postural control (Stapley and Drew, 2009) and locomotion (Dyson et al., 2014). In humans, the PMRF is suggested to participate in locomotor control as well, as it is implicated in anticipatory postural control before gait initiation (Takakusaki, 2013). In neuroimaging studies, the imagery of standing (Jahn et al., 2008) and walking (la Fougère et al., 2010) engaged lateral PMRF corresponding to the area reported here. The PMRF is likely to support the locomotion by integrating descending cortical influences (Takakusaki, 2013) and ascending spinoreticular inputs (Kevetter et al., 1982; Sahara et al., 1990). The functions of the PMRF likely extend beyond locomotion control as its neurons project also to the distal forelimb muscles in non-human primates (Riddle et al., 2009) and are modulated during voluntary reaching (Schepens and Drew, 2004) or finger movements (Hirschauer and Buford, 2015). Our results thus provide further evidence for such convergence of sensory afferent and motor efferent pathways by showing that BOLD response during upper limb movements may be modulated by the lower limb stimulation.

In contrast to the PRMF, there is no anatomical evidence for bottom-up inputs to the pontine nuclei (Nagao, 2004), which have been suggested to serve

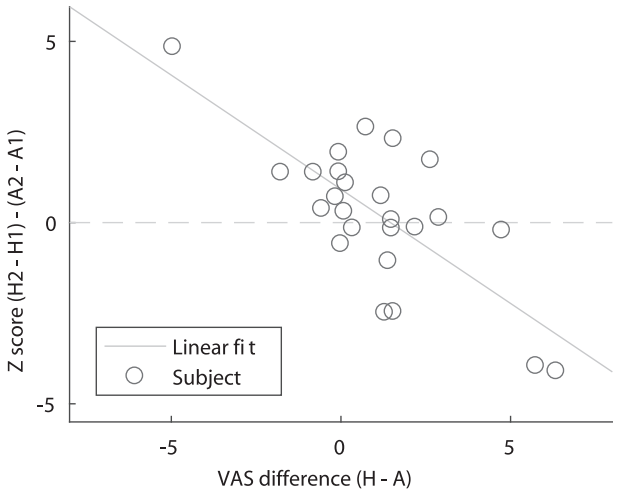

Fig. 4. Correlation with pain intensity. *Black-and-white figure in print.* The scatter plot shows negative correlation between the self-reported pain intensity difference (H–A) and the within-subject interaction (H1–H2 > A1–A2) represented by *Z* scores extracted from the pain effect cluster in the right frontal operculum and insula (contrast 5). Each circle represents a single subject, while the solid line represents the least-squares linear fit.

merely as a relay station between the cerebral cortex of the same side and contralateral cerebellum (Nagao, 2004).

Cerebellum

The peripheral stimulation modulated activation mainly in the lobule VIII and IX. Both lobuli are known to receive spinal inputs (Brodal and Jansen, 1941), either via bilateral spinocerebellar tracts (Yaginuma and Matsushita, 1989) or via the lateral reticular nucleus, which has been suggested to integrate multimodal inputs from spinal afferents and spinal locomotor centers (Alstermark and Ekerot, 2013). In patients, lesions of the spinocerebellum lead to dyscoordination of upright posture and gait (Ilg et al., 2008). However, lobule IX is also implicated in oculomotor control and postural orientation in space and receives vestibulocerebellar fibers and cortical inputs via the contralateral pontine nuclei (Voogd et al., 2012).

The posterior cerebellum is also involved in sensorimotor circuits related to upper extremities, e.g., during finger tapping task (Stoodley et al., 2012). Meta-analyses of functional imaging studies showed overlapping motor and somatosensory activations in the lobule VIII, suggesting a prominent role in the sensorimotor integration (Riedel et al., 2015).

By combining the previous functional and anatomical evidence with our observations, we suggest that, first, the PMRF and posterior cerebellar areas interact during the motor performance within a common reticulocerebellar network, possibly integrating cortical and peripheral inputs. Second, this network may be transiently up-regulated in response to specific peripheral stimulation. In this circuit, the PMRF may serve both as the primary input and output node since it receives direct spinal inputs (Kevetter et al., 1982; Sahara et al., 1990) and can potentially elicit complex motor responses via the reticulospinal tract (Hirschauer and Buford, 2015).

Correlation with the pain intensity difference

The peripheral stimulation according to Vojta is known to be associated with concomitant pain (Müller, 1974), and indeed, the heel stimulation was perceived more painful than the ankle stimulation in our study. Previous studies employing painful cutaneous pressure stimulation have shown pain-related activations in the primary motor cortex and brainstem that were not present during neutral stimulation (Rolls et al., 2003). The occasionally observed involvement of cortical motor areas during acute pain perception may be possibly associated with the withdrawal response to pain (Apkarian et al., 2005). In contrast, our data reveal a correlation between the complex interaction in task-related activation and the difference in post hoc self-rated pain intensity (VAS). A closer inspection reveals that the motor-related activation in the left anterior insula/frontal operculum decreased after a more painful stimulation (Fig. 4). The contralateral anterior insula has been shown to activate during hand motor performance (Sauvage et al., 2011) and has been mostly considered as a multimodal associative area (Kurth et al., 2010). The preceding painful stimulation may therefore affect the background cognitive processes during the motor task, possibly lowering the subject's attention and engagement in the task.

Implications for the reflex locomotion physiotherapy

Our findings might indicate what structures are involved in the modulatory after-effects of the stimulation according to Vojta (1973), such as facilitation of voluntary movements outlasting the stimulation (Laufens et al., 1995). These immediate effects have been observed to persist for at least 30 min (Vojta and Peters, 2007). It has been speculated that the facilitation does not reflect the primary stimulation but rather a secondary effect resulting from the evoked global motor activation, contraction of numerous muscles associated with massive proprioceptive stimulation, which in turn promotes further facilitation of voluntary movements (Vojta, 1973). In our paradigm, muscle contractions and the associated proprioception were minimal and the observed differential modulation likely reflected other mechanisms.

The efferent pathways mediating the motor response to the stimulation according to Vojta have been speculated to involve the non-pyramidal system (Vojta, 1973). Due to the complex nature of the evoked postural changes, a common coordination supraspinal center has been suggested, most likely midbrain (Vojta, 1973; Laufens et al., 1991). Although the midbrain is believed to contain a midbrain locomotor center (MLR) that plays a key role in human locomotion (Takakusaki and Nozu, 2016), we did not observe any specific changes in that area. Instead, the site-specific modulation of task-related fMRI activity was revealed in the bilateral PMRF, a structure involved both in locomotion (Jahn et al., 2008; la Fougère et al., 2010; Takakusaki, 2013; Dyson

et al., 2014) and postural control (Stapley and Drew, 2009; Takakusaki, 2013). Moreover, the PMRF has already been shown to mediate various asymmetric reflex movement patterns, including the asymmetric tonic neck reflex (Dyson et al., 2014; Hirschauer and Buford, 2015; Takakusaki and Nozu, 2016) that can also be observed in healthy humans and patients with brain lesions (Magnus and de Kleijn, 1912) and shares some similarities with the motor responses observed during stimulation according to Vojta (1973). The provided data are therefore highly suggestive that the PMRF could be directly associated with the effects of the therapeutic stimulation according to Vojta (1973).

Limitations

The spatial resolution of the BOLD data may limit any detailed assignment of activation foci to a single anatomical region in a small structure such as the brainstem. However, brainstem imaging was successfully performed in the past using hardware specifications and spatial resolution similar to ours (Jahn et al., 2008). Additionally, even though higher field 3T scanners might provide better signal-to-noise ratio, data acquisition using a 1.5T scanner may be less prone to magnetic susceptibility artifacts.

Another concern may arise regarding the influence of motion artifacts on the main results. We have demonstrated that the main interaction effect remained significant after advanced de-noising procedures (Pruim et al., 2015b). Whereas removal of residual motion artifact has been strongly recommended for resting-state connectivity analyses (Muschelli et al., 2014), block design analysis may suffer from a decrease in sensitivity to true activations (Johnstone et al., 2006).

Despite a highly sophisticated approach implemented in the ICA-AROMA (Pruim et al., 2015b), we are concerned that the method may introduce another bias that may specifically affect brainstem regions. One of the image features exploited by the ICA-AROMA to detect a noisy signal component is the overlap of the independent component with a brain edge mask. Since the edge mask is defined as a 10-mm outer layer of the brain mask, we would expect that some neuronal signal sources might be erroneously removed from the data.

Finally, studies demonstrating the effect of additional removal of suspected motion-related signals (Muschelli et al., 2014; Pruim et al., 2015a) have shown the benefit for lower level group contrasts. However, for higher level contrasts such as group-by-time interaction used in our analysis, the additional preprocessing pipelines, including ICA-based denoising, have yielded rather heterogeneous results and may introduce a substantial bias (Churchill et al., 2012). For these reasons, we decided to primarily present the original data analysis.

CONCLUSIONS

We have shown that sustained pressure stimulation of the foot was associated with differential short-term changes in hand motor task-related activation that depended on the site of stimulation. These differential responses were located in the brainstem and cerebellum, namely in the bilateral, but predominantly contralateral pontomedullary reticular formation and bilateral posterior cerebellar hemisphere and vermis. We propose that the pontomedullary reticular formation, previously implicated in the postural control and generation of asymmetric motor patterns, might be specifically modulated by the pressure stimulation according to Vojta.

GLOSSARY

Vojta physiotherapy (reflex locomotion physiotherapy) – a therapeutic procedure used in several world countries that involves involuntary tonic motor responses elicited by manual pressure applied at certain body surface areas and is known to facilitate voluntary movements and improve motor deficits post-stimulation.

Acknowledgments—The authors thank Dr. Ana Solodkin for valuable comments on an earlier version of this manuscript.

Funding: This work was supported by grant of the Czech Science Foundation (GACR) [grant number 14–22572S].

REFERENCES

Alstermark B, Ekerot C-F (2013) The lateral reticular nucleus: a precerebellar centre providing the cerebellum with overview and integration of motor functions at systems level. A new hypothesis. J Physiol 591:5453–5458.

Apkarian AV, Bushnell MC, Treede R-D, Zubieta J-K (2005) Human brain mechanisms of pain perception and regulation in health and disease. Eur J Pain 9:463–484.

Brodal A, Jansen J (1941) [Beitrag zur Kenntnis der spino-cerebellaren Bahnen beim Menschen]. Anat Anz 91:185–195.

Chipchase LS, Schabrun SM, Hodges PW (2011) Peripheral electrical stimulation to induce cortical plasticity: a systematic review of stimulus parameters. Clin Neurophysiol 122:456–463.

Churchill NW, Yourganov G, Oder A, Tam F, Graham SJ, Strother SC (2012) Optimizing preprocessing and analysis pipelines for single-subject fMRI: 2. Interactions with ICA, PCA, task contrast and inter-subject heterogeneity. PLoS One 7:e31147.

D'Ascanio P, Gahéry Y, Pompeiano O, Stampacchia G (1986) Effects of pressure stimulation of the body surface on posture and vestibulospinal reflexes. Arch Ital Biol 124:43–63.

Desikan RS, Ségonne F, Fischl B, Quinn BT, Dickerson BC, Blacker D, Buckner RL, Dale AM, Maguire RP, Hyman BT, Albert MS, Killiany RJ (2006) An automated labeling system for subdividing the human cerebral cortex on MRI scans into gyral based regions of interest. Neuroimage 31:968–980.

Diedrichsen J, Maderwald S, Küper M, Thürling M, Rabe K, Gizewski ER, Ladd ME, Timmann D (2011) Imaging the deep cerebellar nuclei: a probabilistic atlas and normalization procedure. Neuroimage 54:1786–1794.

Dyson KS, Miron J-P, Drew T (2014) Differential modulation of descending signals from the reticulospinal system during reaching and locomotion. J Neurophysiol 112:2505–2528.

Eickhoff SB, Paus T, Caspers S, Grosbras M-H, Evans AC, Zilles K, Amunts K (2007) Assignment of functional activations to probabilistic cytoarchitectonic areas revisited. Neuroimage 36:511–521.

Foerster O (1933) The dermatomes in man. Brain 56:1–39.

Gallasch E, Christova M, Kunz A, Rafolt D, Golaszewski S (2015) Modulation of sensorimotor cortex by repetitive peripheral magnetic stimulation. Front Hum Neurosci 9.

Golaszewski SM, Siedentopf CM, Koppelstaetter F, Rhomberg P, Guendisch GM, Schlager A, Gallasch E, Eisner W, Felber SR, Mottaghy FM (2004) Modulatory effects on human sensorimotor

cortex by whole-hand afferent electrical stimulation. Neurology 62:2262–2269.
Grabner G, Janke AL, Budge MM, Smith D, Pruessner J, Collins DL (2006) Symmetric atlasing and model based segmentation: an application to the hippocampus in older adults. Med Image Comput Comput Assist Interv 9:58–66.
Grillner S, Wallén P (1985) Central pattern generators for locomotion, with special reference to vertebrates. Annu Rev Neurosci 8:233–261.
Hirschauer TJ, Buford JA (2015) Bilateral force transients in the upper limbs evoked by single-pulse microstimulation in the pontomedullary reticular formation. J Neurophysiol 113:2592–2604.
Hongo T, Kudo N, Oguni E, Yoshida K (1990) Spatial patterns of reflex evoked by pressure stimulation of the foot pads in cats. J Physiol 420:471–487.
Ilg W, Giese MA, Gizewski ER, Schoch B, Timmann D (2008) The influence of focal cerebellar lesions on the control and adaptation of gait. Brain 131:2913–2927.
Jahn K, Deutschländer A, Stephan T, Kalla R, Wiesmann M, Strupp M, Brandt T (2008) Imaging human supraspinal locomotor centers in brainstem and cerebellum. Neuroimage 39:786–792.
Jenkinson M, Beckmann CF, Behrens TEJ, Woolrich MW, Smith SM (2012) FSL. Neuroimage 62:782–790.
Johnstone T, Ores Walsh KS, Greischar LL, Alexander AL, Fox AS, Davidson RJ, Oakes TR (2006) Motion correction and the use of motion covariates in multiple-subject fMRI analysis. Hum Brain Mapp 27:779–788.
Joyce CR, Zutshi DW, Hrubes V, Mason RM (1975) Comparison of fixed interval and visual analogue scales for rating chronic pain. Eur J Clin Pharmacol 8:415–420.
Kavounoudias A, Roll R, Roll J-P (2001) Foot sole and ankle muscle inputs contribute jointly to human erect posture regulation. J Physiol 532:869–878.
Kevetter GA, Haber LH, Yezierski RP, Chung JM, Martin RF, Willis WD (1982) Cells of origin of the spinoreticular tract in the monkey. J Comp Neurol 207:61–74.
Kincses ZT, Johansen-Berg H, Tomassini V, Bosnell R, Matthews PM, Beckmann CF (2008) Model-free characterization of brain functional networks for motor sequence learning using fMRI. Neuroimage 39:1950–1958.
Kurth F, Zilles K, Fox PT, Laird AR, Eickhoff SB (2010) A link between the systems: functional differentiation and integration within the human insula revealed by meta-analysis. Brain Struct Funct 214:519–534.
la Fougère C, Zwergal A, Rominger A, Förster S, Fesl G, Dieterich M, Brandt T, Strupp M, Bartenstein P, Jahn K (2010) Real versus imagined locomotion: A [^{18}F]-FDG PET-fMRI comparison. Neuroimage 50:1589–1598.
Laufens G, Seitz S, Staenicke G (1991) Vergleichend biologische Grundlagen zur angeborenen Lokomotion insbesondere zum "reflektorischen Kriechen" nach Vojta. Z Physiother 43:448–456.
Laufens G, Poltz W, Jugelt E, Prinz E, Reimann G, Van Slobbe T (1995) Motor improvements in multiple-sclerosis patients by Vojta physiotherapy and the influence of treatment positions. Phys Med Rehabilit Kurortmed 5:115–119.
Lim H, Kim T (2013) Effects of vojta therapy on gait of children with spastic diplegia. J Phys Ther Sci 25:1605–1608.
Magnus R, de Kleijn A (1912) [Die Abhängigkeit des Tonus der Extremitätenmuskeln von der Kopfstellung]. Pflügers Archiv Eur J Physiol 145:455–548.
Müller H (1974) Comment on V. Vojta's: early diagnosis and therapy of cerebral disturbances of motility in infancy (author's transl). Z Orthop Ihre Grenzgeb 112:361–364.
Muschelli J, Nebel MB, Caffo BS, Barber AD, Pekar JJ, Mostofsky SH (2014) Reduction of motion-related artifacts in resting state fMRI using aCompCor. Neuroimage 96:22–35.
Nagao S (2004) Pontine nuclei-mediated cerebello-cerebral interactions and its functional role. Cerebellum 3:11–15.
Nieuwenhuys R, Voogd J, Huijzen C van (2008) The human central nervous system. Berlin; New York: Springer.
Oldfield RC (1971) The assessment and analysis of handedness: the Edinburgh inventory. Neuropsychologia 9:97–113.
Powell J, Pandyan AD, Granat M, Cameron M, Stott DJ (1999) Electrical stimulation of wrist extensors in poststroke hemiplegia. Stroke 30:1384–1389.
Pruim RHR, Mennes M, Buitelaar JK, Beckmann CF (2015a) Evaluation of ICA-AROMA and alternative strategies for motion artifact removal in resting state fMRI. Neuroimage 112:278–287.
Pruim RHR, Mennes M, van Rooij D, Llera A, Buitelaar JK, Beckmann CF (2015b) ICA-AROMA: a robust ICA-based strategy for removing motion artifacts from fMRI data. Neuroimage 112:267–277.
Riddle CN, Edgley SA, Baker SN (2009) Direct and indirect connections with upper limb motoneurons from the primate reticulospinal tract. J Neurosci 29:4993–4999.
Riedel MC, Ray KL, Dick AS, Sutherland MT, Hernandez Z, Fox PM, Eickhoff SB, Fox PT, Laird AR (2015) Meta-analytic connectivity and behavioral parcellation of the human cerebellum. Neuroimage 117:327–342.
Rolls ET, O'Doherty J, Kringelbach ML, Francis S, Bowtell R, McGlone F (2003) Representations of pleasant and painful touch in the human orbitofrontal and cingulate cortices. Cereb Cortex 13:308–317.
Rosenkranz K, Rothwell JC (2003) Differential effect of muscle vibration on intracortical inhibitory circuits in humans. J Physiol 551:649–660.
Sahara Y, Xie YK, Bennett GJ (1990) Intracellular records of the effects of primary afferent input in lumbar spinoreticular tract neurons in the cat. J Neurophysiol 64:1791–1800.
Sauvage C, Poirriez S, Manto M, Jissendi P, Habas C (2011) Reevaluating brain networks activated during mental imagery of finger movements using probabilistic Tensorial Independent Component Analysis (TICA). Brain Imag Behav 5:137–148.
Schepens B, Drew T (2004) Independent and convergent signals from the pontomedullary reticular formation contribute to the control of posture and movement during reaching in the cat. J Neurophysiol 92:2217–2238.
Sharp FR, Ryan AF (1984) Regional (^{14}C) 2-deoxyglucose uptake during forelimb movements evoked by rat motor cortex stimulation: pons, cerebellum, medulla, spinal cord, muscle. J Comp Neurol 224:286–306.
Solodkin A, Hluštík P, Noll DC, Small SL (2001) Lateralization of motor circuits and handedness during finger movements. Eur J Neurol 8:425–434.
Stapley PJ, Drew T (2009) The pontomedullary reticular formation contributes to the compensatory postural responses observed following removal of the support surface in the standing cat. J Neurophysiol 101:1334–1350.
Steele CJ, Penhune VB (2010) Specific increases within global decreases: a functional magnetic resonance imaging investigation of five days of motor sequence learning. J Neurosci 30:8332–8341.
Stoodley CJ, Valera EM, Schmahmann JD (2012) Functional topography of the cerebellum for motor and cognitive tasks: an fMRI study. Neuroimage 59:1560–1570.
Takakusaki K, Chiba R, Nozu T, Okumura T (2016) Brainstem control of locomotion and muscle tone with special reference to the role of the mesopontine tegmentum and medullary reticulospinal systems. J Neural Transm 123:695–729.
Takakusaki K (2013) Neurophysiology of gait: From the spinal cord to the frontal lobe. Mov Disord 28:1483–1491.
Ueno T, Inoue M, Matsuoka T, Abe T, Maeda H, Morita K (2010) Comparison between a real sequential finger and imagery movements: an fMRI study revisited. Brain Imag Behav 4:80–85.
Vojta V, Peters A (2007) [Das Vojta-Prinzip: Muskelspiele in Reflexfortbewegung und motorischer Ontogenese]. 3. vollst. überarb. Aufl. Berlin: Springer.
Vojta V (1973) Early diagnosis and therapy of cerebral movement disorders in childhood. C. Reflexogenous locomotion-reflex creeping and reflex turning. C1. The kinesiologic content and

connection with the tonic neck reflexes. Z Orthop Ihre Grenzgeb 111:268–291.
Voogd J, Schraa-Tam CKL, van der Geest JN, De Zeeuw CI (2012) Visuomotor cerebellum in human and nonhuman primates. Cerebellum 11:392–410.
Winkler AM, Ridgway GR, Webster MA, Smith SM, Nichols TE (2014) Permutation inference for the general linear model. Neuroimage 92:381–397.
Woolrich MW, Behrens TEJ, Beckmann CF, Jenkinson M, Smith SM (2004) Multilevel linear modelling for FMRI group analysis using Bayesian inference. Neuroimage 21:1732–1747.
Worsley KJ (2001) Statistical analysis of activation images. In: Jezzard P, Matthews PM, Smith SM, editors. Functional MRI: An Introduction to Methods. Oxford [England]; New York: Oxford University Press.
Wu CW-H, van Gelderen P, Hanakawa T, Yaseen Z, Cohen LG (2005) Enduring representational plasticity after somatosensory stimulation. Neuroimage 27:872–884.
Yaginuma H, Matsushita M (1989) Spinocerebellar projections from the upper lumbar segments in the cat, as studied by anterograde transport of wheat germ agglutinin-horseradish peroxidase. J Comp Neurol 281:298–319.

(Received 5 October 2016, Accepted 5 February 2017)
(Available online 14 February 2017)